HETEROGENEOUS OXYGEN ISOTOPIC COMPOSITIONS IN A SAPPHIRINE-BEARING AL-RICH CHONDRULE FROM THE DAG 978 CARBONACEOUS CHONDRITE. A. C. Zhang[1,2], S. Itoh[2], N. Sakamoto[3], R. C. Wang[1], and H. Yurimoto[2,3], [1]School of Earth Sciences and Engineering, Nanjing University, China; [2]Department of Natural History Sciences, Hokkaido University, Japan; [3]Isotope Imaging Laboratory, CRIS, Hokkaido University, Japan.

Introduction: Aluminum-rich chondrules are chondrules with >10 wt% bulk Al_2O_3 contents [1]. They provide important clues to understand the genetic relationship between Ca,Al-rich inclusions and ferromagnesian chondrules. Previous investigations suggested that some Al-rich chondrules if not all could have formed by melting of hybrid mixtures of ferromagnesian chondrules and CAIs [2,3]. However, given the high bulk Al_2O_3 contents, this model cannot explain the ^{16}O-poor oxygen isotopic features in most Al-rich chondrules (e.g., [4,5]). To interpret the ^{16}O-poor oxygen isotopic compositions of Al-rich chondrules, some investigators proposed that ^{16}O-rich, Al-rich melt experienced oxygen isotopic exchange with ^{16}O-poor nebular gas before solidification (e.g., [6]). However, without other strong evidence indicating a mixing origin for Al-rich chondrules, the oxygen isotopic exchange model itself is not a convincing interpretation. To further understand the origin of Al-rich chondrules, we measured REE compositions and oxygen isotopic compositions in a sapphirine-bearing Al-rich chondrule (abbreviated as SARC) in a type 3 carbonaceous chondrite DaG 978. With these data, we discuss the possible origin of oxygen isotopic distribution in SARC.

Results: SARC has a core-mantle-rim texture. Both the core (~700 μm in diameter) and the mantle (~400 μm in thickness) are Al-rich (>20 wt% Al_2O_3) and mainly consist of Al-rich protoenstatite (8-11 wt% Al_2O_3) and anorthite (An_{82-89}). The characteristics are: 1) The core contains abundant Fe-rich spinel (Mg# = 58-60) grains (up to 15 μm in size). 2) The mesostasis in the core contain euhedral sapphirine prisms ($Mg_2Al_4SiO_{10}$). 3) A few Fe-rich olivine (Mg# = 68-71) and Fe-Ni metal grains occur in the mantle. 4) Besides very fine-grained Fe-rich diopside and anorthite, some mesostasis of the mantle also contains enstatite grains, which have lower Al_2O_3 contents (down to 3.7 wt%) and higher FeO contents (up to 14 wt%) than those of relatively coarse Al-rich enstatite. 5) Some fractures in the mantle anorthite are filled by nepheline. The rim of SARC consists of olivine (Mg# = 69), Al-poor enstatite (~1 wt% Al_2O_3), and Fe-Ni metal, similar in texture and mineralogy to those in POP chondrules.

Eight REE results on mesostasis measured using a CAMECA IMS-6f SIMS instrument at Hokkaido University [7] show that all mesostasis in SARC are enriched in REE and have a Group II REE pattern with a flat LREE pattern and a fractionated HREE pattern (Fig. 1). But, the REE abundances of mesostasis in the core (La ~220-336 x CI) are generally higher than those of mesostasis in the mantle (La ~140-283 x CI).

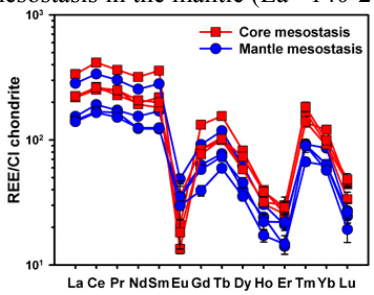

Fig. 1. REE patterns of mesostasis.

The O isotopic compositions of minerals in SARC were measured using a CAMECA IMS-1270 SIMS instrument at Hokkaido University [8]. The results plot along the CCAM line in the oxygen three-isotope diagram. There is no strong relationship between O isotopic compositions and textures (Fig. 2). Spinel is ^{16}O-rich ($\Delta^{17}O$ = –19.9 ‰). Sapphirine and enstatite have similar O isotopic compositions with an average $\Delta^{17}O$ of –6.7 and –6.1 ‰, respectively. Most olivine grains in SARC have similar $\Delta^{17}O$ values to those of sapphirine and enstatite. However, a few analyses on olivine show ^{16}O-rich O isotopic compositions with the $\Delta^{17}O$ down to –23.0 ‰. One olivine grain is almost homogeneously ^{16}O-rich ($\Delta^{17}O$ = –23.0 ‰ to –21.2 ‰). Anorthite and mesostasis (including one 10-μm diopside grain) have similar O isotopic compositions with an average $\Delta^{17}O$ of –2.9 ‰ and –2.3 ‰, respectively.

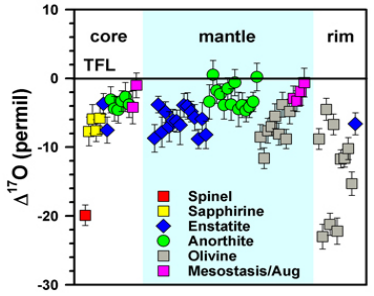

Fig. 2. Oxygen isotopic compositions in SARC minerals.

Discussion: Several independent lines of evidence indicate that precursor of the Al-rich core and mantle could be a mixture of materials from CAI and normal chondrule. 1) The Al-rich core and mantle in SARC is intermediate in bulk chemistry and mineralogy be-

tween CAIs and ferromagnesian chondrules. Olivine and Fe-Ni metal, the common minerals in ferromagnesian chondrules, also occur in the mantle. 2) Both mesostasis from the core and the mantle have Group II REE patterns, which can be explained only by fractional condensation from a nebula where ultrarefractory components have been removed [9,10]. 3) It is well accepted that primitive refractory inclusions are ^{16}O-rich whereas chondrules are ^{16}O-poor (e.g., [11]). So, the ^{16}O-rich feature of spinel in the core is another important piece of evidence supporting that the precursor material of the core in SARC is related to materials from refractory inclusions. The very low abundance of olivine in the Al-rich core and mantle implies that the precursor refractory inclusion is a CAI, not AOAs.

The above discussions strongly indicate that the precursor of the Al-rich portion in SARC is a hybrid mixture of materials from CAI and ferromagnesian chondrule. However, the Al-rich portion in SARC is highly Al-rich, indicating a high proportion of CAI component in the precursor material. So, if there was no oxygen isotope exchange during or after the formation of SARC or on the parent body, most components of the Al-rich portion in SARC should be more ^{16}O-rich than those we observed, which are similar to those of ferromagnesian chondrule component. However, the observation is contrast to this inference. Thus, it is very likely that oxygen isotope exchange occurred during melting of the precursor materials of SARC or after solidification of SARC.

Besides the ^{16}O-rich spinel and olivine, which could be of relict origin, other minerals in SARC generally have two groups of oxygen isotopic compositions: one group (enstatite, sapphirine, and most olivine) has Δ^{17}O of –6.1 to –6.7 ‰; the other group (anorthite and mesostasis) has higher Δ^{17}O (–2.9 to –2.3 ‰). This feature indicates that SARC might have experienced two oxygen isotopic exchange events under independent conditions.

One oxygen isotopic exchange event could have occurred during melting of the precursor of SARC in nebula as other investigations suggested (e.g., [6]). During this exchange event, the ^{16}O-rich hot melt exchanged its oxygen isotopic compositions with surrounding ^{16}O-poor nebular gas, which Δ^{17}O could be around –6.1 to –6.7 ‰. Spinel remained its ^{16}O-rich feature due to its high melting point and the slow diffusivity of oxygen in spinel crystal.

The other oxygen isotopic exchange event probably occurred on the parent body of DaG 978. We modeled the O and Fe-Mg diffusions in different minerals under anhydrous and hydrous conditions (Fig. 3). Oxygen diffusions in spinel and forsterite are considered as the upper limit of temperature and diffusion time. Other diffusions observed in SARC are considered to constrain the lower limit of temperature and diffusion time. A maximum metamorphic temperature (~840 K) of DaG 978 was calculated based on spinel-olivine geothermometry. Under anhydrous conditions, the ^{16}O-poor isotopic feature of diopside cannot be interpreted and an unreasonably long diffusion time (>37 myr) for a parent body of type 3 chondrite would be needed. However, under hydrous conditions, all observed diffusion lengths in SARC can be explained within 3 myr if the metamorphic temperature is up to 840 K. Thus, the diffusion model supports that the second oxygen isotopic exchange event occurred on the parent body under hydrous conditions for minerals of Δ^{17}O = –2.9 to –2.3 ‰.

References: [1] Bischoff A. and Keil K. (1984) *GCA, 48,* 693–709. [2] MacPherson G. J. and Huss G. R. (2005) *GCA*, 69, 3099-3127. [3] Russell S. S. et al. (2005) In *Chondrites and the Protoplanetary Disk*, Pp 317–350. [4] Russell S. S. et al. (2000) *EPSL*, 184, 57–74. [5] Guan Y. B. et al. (2006) *MAPS*, 41, 33–47. [6] Hsu W. B. et al. (2012) *75th Annual Meteoritical Society Meeting*, Abstract#5165. [7] Wang W. Y. and Yurimoto H. (1993). *Ann. Rep. Inst. Geosci., Univ. Tsukuba* 19, 87–91. [8] Yurimoto H. et al. (1998) *Science*, 282, 1874-1877. [9] Boynton W. V. (1975) *GCA*, 39, 569–584. [10] Davis A. M. and Grossman L. (1979) *GCA*, 43, 1611–1632. [11] Yurimoto H. et al. (2008) *RMG*, 68, 141–186.

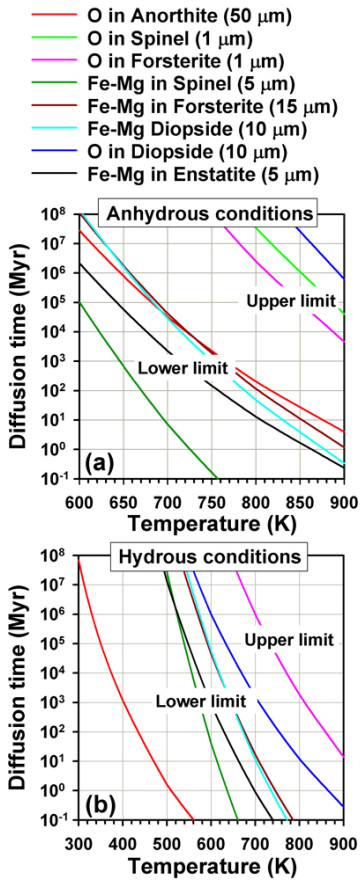

Fig. 3. Modelling of temperature and diffusion time for oxygen and Fe-Mg diffusion in different minerals.